Restructuring effects in irreversible deposition of spheres on a plane

G. Tarjus and P. Viot
Laboratoire de Physique Théorique des Liquides, Université Pierre et Marie Curie, 4, place Jussieu, 75252 Paris Cedex 05, France

H. S. Choi and J. Talbot
School of Chemical Engineering, Purdue University, West Lafayette, Indiana 47907
(Received 23 July 1993)

We present an irreversible-deposition model which encompasses as special cases both random sequential adsorption (RSA) and simple ballistic deposition (BD). In this deposition process, hard spheres are added sequentially to a plane along vertical straight-line trajectories initiated at random positions. Multilayer formation is prevented. The spheres can adsorb on the plane either by direct deposition or by following the path of steepest descent on previously deposited particles. The ratio of the rates of the two mechanisms is characterized by a parameter which is equal to 0 for RSA and 1 for simple BD. Using liquid-state methods, we obtain a third-order density expansion for the pair-density function and for the rate of deposition. We consider also the kinetics of the process and we show, by computer simulation and theoretical arguments, that the system reaches its saturation state exponentially. Finally, we discuss several interpolation formulas that incorporate the exact small- and large-time behavior.

PACS number(s): 81.15.Lm

I. INTRODUCTION

Models of irreversible deposition in monolayers have attracted significant theoretical effort and are useful in the interpretation of experimental studies such as the adsorption of large molecules on solid surfaces [1–6]. Colloidal and biological particles, like proteins, bacteria, and viruses, adsorb at liquid-solid interfaces with negligible desorption and surface diffusion on the time scale of observation. A well-known example of an irreversible monolayer deposition process is the random sequential adsorption (RSA) [7]. In the prototypical version of this model, hard objects are deposited sequentially on a surface. Their positions are chosen at random, and each particle excludes a certain area from additional particles. Although RSA takes into account geometrical exclusion effects and the irreversible nature of the process, the systematic rejection of those particles that overlap with previously adsorbed particles appears to be a strong limitation of the model.

A quantitative description of the adsorption mechanism must include the transport of the particles from bulk to the surface. This requires knowledge of the different interactions involved in the process which may include dispersion, electrostatic, hydrodynamic forces, and possibly external fields, such as gravity, in addition to the short-range repulsion. An interesting approach that incorporates some features of the transport mechanism consists of allowing the particles to undergo a Brownian motion in solution under the influence of these forces.

If the density of the adsorbing particles is approximately equal to that of the solvent, gravity forces can be neglected and a pure diffusional motion can be considered; this corresponds to the diffusion RSA (DRSA) model introduced by Schaaf, Johner, and Talbot [8]. From a simulation study of the $(2+1)$-dimensional system, Senger *et al.* [9–11] pointed out that the kinetics of the DRSA are significantly different from those of the RSA but that the coverage and the monolayer structure at saturation are extremely close to those obtained by the RSA model. Tarjus and Viot [12] showed that a large class of generalized car parking problems have the same jamming limit as the simple parking [or one-dimensional (1D) RSA] model, and that the $(1+1)$-dimensional DRSA process can be well approximated by a generalized parking process.

Conversely, if the adsorbing particles are denser than the solvent, the motion of the particle is dominated by a significant drift toward the surface due to the gravitational force [13]. In the limit of a very large density difference the motion of the heavy particles can be described by straight-line trajectories in solution and near the absorbing surface by the path of steepest descent on the previously adsorbed particles. Talbot and Ricci [14] obtained an analytical solution of a $(1+1)$-dimensional version of this ballistic deposition model in which multilayer formation is not allowed. Jullien and Meakin [15], Thompson and Glandt [16], and Choi *et al.* [17] investigated the same model in $(2+1)$ dimensions by computer simulation. A comparison between RSA and ballistic-deposition (BD) models reveals that BD saturation coverage is larger than RSA saturation coverage, and that the saturation state is reached faster in the BD model (exponential instead of algebraic time behavior); finally, the cooperative restructuring effects, which represent the possibility for a trial sphere to move over one or more neighboring preadsorbed spheres in order to reach the plane, contribute to the formation of connected clusters.

In this paper, we study a modified $(2+1)$-dimensional ballistic-deposition model, which encompasses RSA and BD as special cases. This model, corresponding to sequential deposition of hard spheres of diameter σ (σ is

 ©1994 The American Physical Society

chosen as unit length in the following) onto an infinite adsorbing plane, is defined as follows. Starting from an arbitrary horizontal plane above the adsorbing plane, the spheres, which are randomly positioned, are dropped at a rate k and follow vertical trajectories until they reach (i) the adsorbing plane or (ii) a preadsorbed sphere. In case (i), the trial sphere is placed definitively with a probability p or removed with a probability $(1-p)$. In case (ii), the trial sphere follows the path of steepest descent on the previously adsorbed particles: if the particle is trapped in a stable position without contacting the adsorbing plane, it is removed (no multilayer formation); otherwise, the particle reaches the plane, and it is clamped with a probability p' or is rejected with a probability $(1-p')$. With the introduction of the dimensionless variables $t=kp\tau$, where τ is the number of attempts per unit area, and $a=p'/p$, the kinetics of the process is governed by the evolution equation

$$\frac{\partial\rho(a,t)}{\partial t}=\Phi(a,\rho) , \tag{1}$$

where $\Phi(a,\rho)$ is the rate of deposition on the surface for a new sphere when the density of adsorbed spheres is equal to $\rho\equiv\rho(a,t)$.

The tuning parameter a controls the efficiency of the restructuring. The switch-off of this parameter corresponds to the RSA model, whereas for $a=1$ one recovers the simple BD model. For $0<a<1$, this model mimics the physical situations in which adsorption is partially influenced by gravity: a increases with increasing density difference between the particle and solution. For very large values of a, the model describes island or grain growth [7]. In this case, the value of a controls the ratio of grain growth to the seeding of new grains. In all cases, an increasing of the tuning parameter a leads to more efficient space filling and significant changes of the structure. Kinetics and cluster densities have been obtained for the $(1+1)$-dimensional version of this model (deposition of disks on a line) [18]. As for RSA processes, no analytical solution can be found over the entire coverage range in higher dimensions, but using liquid-state methods [16,19,20], we derive in Sec. II the third-order density expansion of the rate of deposition and of the pair density function for the $(2+1)$-dimensional process. In Sec. III, we show that the asymptotic approach of the coverage towards the saturation state (jamming limit) is exponential for $a>0$, and we study the crossover between power-law and exponential behavior at small values of a. A numerical investigation of this model is presented in Sec. IV, and the data from simulation are compared to the results of the previous sections. Finally, several approximate interpolation formulas that incorporate the exact small- and large-time behavior are discussed.

II. LOW-DENSITY EXPANSION

The density of adsorbed spheres increases monotonically with time due to the two possibilities to add a new sphere, either by direct deposition (DD) or by the rolling mechanism (RM). Thus, the rate of deposition $\Phi(a,\rho)$ can be expressed formally as

$$\Phi(a,\rho)=\Phi^{\mathrm{DD}}(a,\rho)+a\Phi^{\mathrm{RM}}(a,\rho) , \tag{2}$$

where $\Phi^{\mathrm{DD}}(a,\rho)$ and $\Phi^{\mathrm{RM}}(a,\rho)$ are the probability for a new particle to reach the surface by direct deposition or by rolling mechanism, respectively. $\Phi^{\mathrm{DD}}(a,\rho)$ and $\Phi^{\mathrm{RM}}(a,\rho)$ depend on the configuration of already adsorbed spheres when their density is equal to ρ. This configuration can be considered as an arrangement of two-dimensional (2D) disks of diameter $\sigma=1$ and the $(2+1)$-dimensional process can be reduced to a 2D process with restructuring. Then, as in RSA, $\Phi^{\mathrm{DD}}(a,\rho)$ can be interpreted as the fraction of the total surface that is accessible to the center of a new particle without overlap with preadsorbed spheres. Moreover, because of the macroscopic uniformity of the system, $\Phi^{\mathrm{RM}}(a,\rho)$ is also the complementary fraction of the sum of the relative area available for direct deposition and that available for second layer formation; it can be written as

$$\Phi^{\mathrm{RM}}(a,\rho)=1-\Phi^{\mathrm{DD}}(a,\rho)-\Psi(a,\rho) , \tag{3}$$

where $\Psi(a,\rho)$ denotes the relative area of the region in which a trial particle can be trapped in an elevated position without reaching the adsorbing surface and could then participate, if it were not prevented, in the formation of a second layer. Using Eqs. (2) and (3), the rate of deposition is then given by

$$\Phi(a,\rho)=(1-a)\Phi^{\mathrm{DD}}(a,\rho)+a(1-\Psi(a,\rho)) . \tag{4}$$

Also, because of the macroscopic uniformity of the monolayer, $\Phi^{\mathrm{DD}}(a,\rho)$ represents the probability that around any point $\mathbf{r}_1$, there is a disk of diameter 2σ that is free from any center of previously adsorbed spheres, and this leads to the following expression [19]:

$$\begin{aligned}\Phi^{\mathrm{DD}}(a,\rho)&=\sum_{s=0}^{\infty}\frac{\rho^s}{s!}\int\cdots\int d2\cdots d(s+1)f_{12}\cdots f_{1(s+1)}g_s(2\cdots(s+1);a,\rho)\\&=\sum_{s=0}^{\infty}\frac{\rho^s}{s!}\int\cdots\int d2\cdots d(s+1)\left[\frac{1}{S}\int d1 f_{12}\cdots f_{1(s+1)}\right]g_s(2\cdots(s+1);a,\rho) ,\end{aligned} \tag{5}$$

where S is the total surface area, f denotes a Mayer function for hard disks, and $g_s(2,3,\ldots,(s+1);a,\rho)$ is the s-particle distribution function.

Using geometrical and probabilistic arguments, one can obtain a formal expression for $\Psi(a,\rho)$:

$$\Psi(a,\rho)=\sum_{s=3}^{\infty}\frac{\rho^s}{s!}\int\cdots\int d2\,d3\cdots d(s+1)A(2,3,\ldots,(s+1))g_s(2,3,\ldots,(s+1);a,\rho) , \tag{6}$$

where $A(2,3,\ldots,(s+1))$ denotes the area of the polygon that has $2, 3, \ldots, (s+1)$ for vertices and is such that any center of particle falling in it reaches a unique elevated position above the surface. By convention, A is zero when no stable elevated position is found.

We now investigate the short-time kinetics and the low-density structure by calculating the density expansion of the pair-distribution function $g_2(1,2;a,\rho)$ and that of the rate of deposition $\Phi(a,\rho)$. The kinetic equations, (1) and (2), can be generalized for higher-order distribution functions, by applying arguments similar to those introduced by Tarjus, Schaaf, and Talbot [19] for RSA. For example, $\rho^2 g_2(1,2;a,\rho)d1\,d2$ is equal to the probability that the centers of two (unlabeled) particles are located in $d\mathbf{r}_1$ and $d\mathbf{r}_2$ around $\mathbf{r}_1$ and $\mathbf{r}_2$, respectively. Between times t and $t+dt$, new pairs can appear by the insertion of a sphere at the point $\mathbf{r}_2$, given that a preadsorbed sphere is at the point $\mathbf{r}_1$, or by the insertion of a sphere at the point $\mathbf{r}_1$, given that a preadsorbed sphere is at the point $\mathbf{r}_2$. The time evolution of the pair-distribution function is then

$$\frac{\partial \rho^2 g_2(1,2;a,\rho)}{\partial t} = [\Phi^{1|2}(1,2;a,\rho)+\Phi^{2|1}(1,2;a,\rho)] , \quad (7)$$

where $\Phi^{1|2}(1,2;a,\rho)$ represents the probability density of finding a particle centered at $\mathbf{r}_1$ and a cavity centered at $\mathbf{r}_2$ such that one particle center can be placed at $\mathbf{r}_2$ either by direct deposition or by rolling mechanism,

$$\Phi^{1|2}(1,2;a,\rho)=\Phi^{1|2(\mathrm{DD})}(1,2;a,\rho) + \Phi^{1|2(\mathrm{RM})}(1,2;a,\rho) . \quad (8)$$

Because the density is a monotonically increasing function of time, there is a one-to-one mapping between t in the range $[0,+\infty[$ and ρ in the range $[0,\rho(+\infty)[$; the time dependence of the equation (7) can be eliminated, yielding

$$\frac{\partial \rho^2 g_2(1,2;a,\rho)}{\partial \rho} = [\Phi^{1|2}(1,2;a,\rho) + \Phi^{2|1}(1,2;a,\rho)]\frac{1}{\Phi(a,\rho)} . \quad (9)$$

Using the derivation of Ref. [19], $\Phi^{1|2(\mathrm{DD})}(1,2;a,\rho)$ takes the form

$$\Phi^{1|2(\mathrm{DD})}(1,2;a,\rho)=(1+f_{12})\sum_{s=0}^{\infty}\frac{\rho^{s+1}}{s!}\int\cdots\int d3\cdots d(s+2) f_{13}\cdots f_{1(s+2)} g_{s+1}(2,3,\ldots,s+2;a,\rho) . \quad (10)$$

However, in contrast to RSA processes, cooperative restructuring effects related to the rolling mechanism lead to nonlocal multiparticle effects, and no simple generic expression has been obtained for $\Phi^{1|2(\mathrm{RM})}(1,2;a,\rho)$. It is possible to obtain the first terms of the expansion by a systematic analysis of all events that lead to a successful adsorption. At the lowest order, a trial particle can be inserted at the location $\mathbf{r}_2$ by rolling on the particle centered in $\mathbf{r}_1$ alone. At the next order, a trial particle can be inserted at $\mathbf{r}_2$, either by rolling on the particle $\mathbf{r}_1$ without contacting particle 3 or by rolling on particles in $\mathbf{r}_1$ and $\mathbf{r}_3$ (see Fig. 1). Consequently, the pair-distribution function has a regular and singular part,

$$g_2(r_{12};a,\rho)=y_2(r_{12};a,\rho)H(r_{12}-1) + g_{2+}(a;\rho)\delta(r_{12}-1) , \quad (11)$$

where H denotes a Heaviside step function. To obtain more tractable expressions, Eq. (9) can be also separated as follows:

$$\frac{\partial}{\partial\rho}\{\rho^2 y_2(r_{12};a,\rho)\}=\frac{2}{\Phi(a,\rho)}[\Phi^{(\mathrm{DD})}(1,2;a,\rho) + \Phi_r^{(\mathrm{RM})}(1,2;a,\rho)] , \quad (12)$$

$$\frac{\partial}{\partial\rho}\{\rho^2 g_{2+}(a,\rho)\}=\frac{2}{\Phi(a,\rho)}\Phi_+^{(\mathrm{RM})}(a,\rho) , \quad (13)$$

where $\Phi_r^{(\mathrm{RM})}(1,2;a,\rho)$ and $\Phi_+^{(\mathrm{RM})}(a,\rho)$ denote, respectively, the regular and singular parts of $\Phi^{(\mathrm{RM})}(1,2;a,\rho)$; we

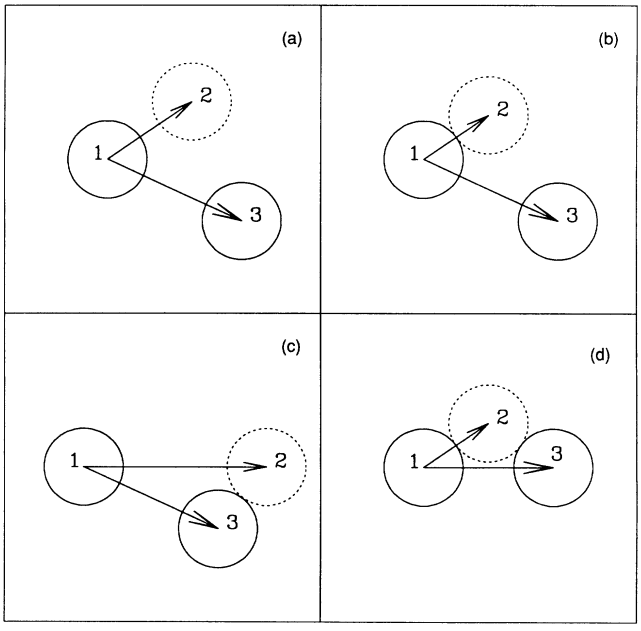

FIG. 1. Illustration of the four possibilities to insert particle 2 in the vicinity of two preadsorbed particles, 1 and 3: (a) particle 2 does not contact 1 and 3, (b) particle 2 contacts 1 but not 3, (c) particle 2 contacts particle 3 but not particle 1, (d) particle 2 contacts both particles 1 and 3; (a) corresponds to a direct deposition and (b), (c), and (d) to the various possibilities involving the rolling mechanism.

have dropped from $\Phi^{(DD)}$ and $\Phi^{(RM)}$ the subscripts $1|2$ and $2|1$ since the contributions are equal.

From Eqs. (4) and (5), the first-order density expansion of $\Phi(a,\rho)$ is given by

$$\Phi(a,\rho)=1-(1-a)\pi\rho+\cdots . \tag{14}$$

From Eq. (10), the direct-deposition contribution can be expressed at second order as

$$\Phi^{DD}(1,2;a,\rho)=\rho+\rho^2\int d3\, f_{13}\left[(1+f_{23})+\frac{a}{2}\delta(r_{23}-1)\right]+\cdots , \tag{15}$$

where we have dropped the factor $(1+f_{12})$ which is equal to $H(r_{12}-1)$ in Eq. (11). After some algebra, one obtains

$$\Phi^{DD}(1,2;a,\rho)=\begin{cases}\rho-\rho^2\left[\pi-(2-a)\cos^{-1}\left[\dfrac{r_{12}}{2}\right]+r_{12}\left[1-\dfrac{r_{12}^2}{4}\right]^{1/2}\right]+\cdots & \text{if } 1\le r_{12}<2 ,\\ \rho-\rho^2\pi+\cdots & \text{if } r_{12}>2 .\end{cases} \tag{16}$$

Note that the piecewise function $\Phi^{(DD)}(1,2;a,\rho)$ is continuous at $r_{12}=2$.

As $\Phi_+^{(RM)}(a,\rho)$ is the sum of contributions due to the adsorption of particle 3 at contact with particle 1 with and without contacting particle 2, the latter itself being in contact with particle 1, one obtains that

$$\Phi_+^{(RM)}(a,\rho)=\tfrac{1}{2}[\rho\Phi^{(DD)}(r_{12}=1;a,\rho)]+\int d3\,\delta(r_{13}-1)[\rho^2 g_2(r_{23};a,\rho=0)]s(r_{12}=1,r_{13}=1,r_{23})+\cdots , \tag{17}$$

where $s(r_{12}=1,r_{13}=1,r_{23})$ denotes the area of the triangle formed by particles 1, 2, and 3, such that any trial particle landing in this triangle follows a steepest descent path which leads to the point $\mathbf{r}_2$. This area can expressed as

$$s(r_{12}=1,r_{13}=1,r_{23})=\frac{r_{23}}{2}\left[1-\frac{r_{23}^2}{4}\right]^{1/2} . \tag{18}$$

Combining Eqs. (17) and (18), it is possible to perform integrations, which gives

$$\Phi_+^{(RM)}(a,\rho)=\rho\left[\tfrac{1}{2}+\rho\left[(1-a)\frac{\pi}{6}+\frac{\sqrt{3}}{8}(2a-1)\right]+\cdots\right] . \tag{19}$$

Let us now consider the adsorption events in which a trial particle can reach the surface in $\mathbf{r}_2$ after rolling over particle 3 without contacting particle 1; $\Phi_r^{(RM)}(1,2;a,\rho)$ is given by

$$\Phi_r^{(RM)}(1,2;a,\rho)=\tfrac{1}{2}\rho^2\int d3\,\delta(r_{13}-1)\times g_2(r_{23};a,\rho=0)+\cdots . \tag{20}$$

After performing the integration, one obtains to the second order in density

$$\Phi_r^{(RM)}(1,2;a,\rho)=\begin{cases}\rho^2\left[\pi-\cos^{-1}\left[\dfrac{r_{12}}{2}\right]+\dfrac{a}{2}\dfrac{1}{r_{12}\left[1-\dfrac{r_{12}^2}{4}\right]^{1/2}}\right] & \\ \text{if } 1\le r_{12}<2 , & \\ \rho^2\pi \quad \text{if } r_{12}>2 . & \end{cases} \tag{21}$$

Hence, collecting the results of Eqs. (16) and (21), the pair-distribution function $g_2(r_{12};a,\rho)$ to order ρ is a piecewise function, such that, if $1\le r_{12}<2$,

$$y_2(r_{12};a,\rho)=1+\tfrac{2}{3}\rho\left\{2(1-a)\cos^{-1}\left[\frac{r_{12}}{2}\right]-r_{12}\left[1-\frac{r_{12}^2}{4}\right]^{1/2}+\frac{a^2}{2}\frac{1}{r_{12}\left[1-\dfrac{r_{12}^2}{4}\right]^{1/2}}\right\} , \tag{22}$$

whereas if $r_{12}>2$,

$$y_2(r_{12};a,\rho)=1 . \tag{23}$$

The singular part of the pair-distribution function is given by

$$g_{2+}(a,\rho)=\frac{a}{2}+\frac{a}{3}\rho\left\{(1-a)\frac{4\pi}{3}+\frac{\sqrt{3}}{4}(2a-1)\right\} . \tag{24}$$

Note that we recover the results already derived for two limiting cases: RSA ($a=0$) [21] and simple BD ($a=1$) [16].

We focus now on the density expansion of the rate of deposition $\Phi(a,\rho)$. It is possible to simplify the calculation by rearranging the terms of the expansion as

$$\Phi(a,\rho)=(1-a)\Phi(a=0,\rho)+(1-a)[\Phi^{DD}(a,\rho)-\Phi(a=0,\rho)]+a(1-\Psi(a,\rho)) , \tag{25}$$

where $\Phi(a=0,\rho)=\Phi^{DD}(a=0,\rho)$ is the RSA available surface function. The third-order density expansion of $\Phi(a=0,\rho)$ has been already derived [21] and recently the fourth-order has been also obtained [22]. Using Eqs. (5) and (6), we can rewrite Eq. (25) as

$$\Phi(a,\rho)-(1-a)\Phi(a=0,\rho)=a+(1-a)\frac{\rho^2}{2}\int\int d2\,d3\,f_{12}f_{13}(g_2^{(0)}(2,3;a)-g_2^{(0)}(2,3;0))$$
$$+\rho^3\left[\frac{(1-a)}{3!}\int\int\int d2\,d3\,d4\,f_{12}f_{13}f_{14}(g_3^{(0)}(2,3,4;a)-g_3^{(0)}(2,3,4;0))\right.$$
$$+\frac{(1-a)}{2!}\int\int d2\,d3\,f_{12}f_{13}(g_2^{(1)}(2,3;a)-g_2^{(1)}(2,3;0))$$
$$\left.-\frac{a}{3!}\int\int\int d2\,d3\,d4\,g_3^{(0)}(2,3,4;a)\frac{A(2,3,4)}{S}\right]+\cdots, \tag{26}$$

where $g_s^{(p)}(2,3,\ldots,s+1;a)$ denotes the pth-order coefficient of the density expansion of the s-particle distribution function.

The expansion of $\Phi(a,\rho)$ up to third order involves the pair-distribution function up to first order and the triplet-distribution function to the zeroth order. It is possible to generalize the arguments that enabled the calculation of the pair-distribution function to higher-order distribution functions. Thus, the triplet-distribution function is given by

$$\frac{\partial\rho^3 g_3(1,2,3;a,\rho)}{\partial\rho}=[\phi^{12|3}(1,2,3;a,\rho)+\Phi^{13|2}(1,2,3;a,\rho)$$
$$+\Phi^{23|1}(1,2;a,\rho)]\frac{1}{\Phi(a,\rho)}, \tag{27}$$

where $\Phi^{12|3}(1,2,3;a,\rho)$ is the probability density of finding two particles at the locations $\mathbf{r}_1$ and $\mathbf{r}_2$ and a cavity at $\mathbf{r}_3$ such that a particle center can be added at the point $\mathbf{r}_3$ either by direct deposition $[\Phi^{12|3(\mathrm{DD})}(1,2,3;a,\rho)]$ or by rolling mechanism $[\Phi^{12|3(\mathrm{RM})}(1,2,3;a,\rho)]$. To the lowest order, the triplet-point-distribution function is equal to

$$g_3^{(0)}(1,2,3;a)=\tfrac{1}{3}[\Phi^{(2)12|3}(1,2,3;a)$$
$$+\Phi^{(2)13|2}(1,2,3;a)$$
$$+\Phi^{(2)23|1}(1,2,3;a)], \tag{28}$$

where the superscript (2) in Φ indicates the second order in the density expansion.

To obtain $\Phi^{(2)12|3}(1,2,3;a,\rho)$, we have to consider the different possibilities for adding a new particle at the location $\mathbf{r}_3$ for a given pair of preadsorbed particles centered at $\mathbf{r}_1$ and $\mathbf{r}_2$: if the two already adsorbed particles are not in contact, $|\mathbf{r}_2-\mathbf{r}_1|>1$, the third particle can be inserted either by direct deposition, i.e., without contact with particle 1 or particle 2, or by rolling over particle 1 or particle 2, or both; if the two already adsorbed particles are in contact $|\mathbf{r}_2-\mathbf{r}_1|=1$, particle 3 can be adsorbed according to the four previous possibilities, and we derive the following expression, at the lowest order in density:

$$\Phi^{(2)12|3}(1,2,3;a,\rho)=\begin{cases}H(r_{12}-1)H(r_{13}-1)H(r_{23}-1)\\ +\frac{a}{2}[\delta(r_{12}-1)H(r_{13}-1)H(r_{23}-1)\\ +H(r_{12}-1)\delta(r_{13}-1)H(r_{23}-1)+H(r_{12}-1)H(r_{13}-1)\delta(r_{23}-1)]\\ +\frac{a^2}{4}\delta(r_{12}-1)[\delta(r_{13}-1)H(r_{23}-1)+H(r_{13}-1)\delta(r_{23}-1)]\\ +\frac{a}{2}\sin^2[\alpha_c(r_{12})]H(r_{12}-1)\delta(r_{13}-1)\delta(r_{23}-1)\\ +\frac{3a^2}{16}\delta(r_{12}-1)\delta(r_{13}-1)\delta(r_{23}-1),\end{cases} \tag{29}$$

where $\alpha_c(r_{12})=\alpha(r_{12},r_{13}=r_{23}=1)$ is the angle between $\mathbf{r}_{31}$ and $\mathbf{r}_{32}$ when $r_{13}=r_{23}=1$ and $1\le r_{12}\le 2$, and $\alpha_c(r_{12})=0$ if $r_{12}\ge 2$. Using Eqs. (11) and (22)–(24), the ρ^2 term of Eq. (26) can be rewritten

$$(1-a)\rho^2\frac{a}{4S}\int\int\int d1\,d2\,d3\,f_{12}f_{13}\delta(r_{23}-1) \tag{30}$$

or

$$(1-a)a\frac{\rho^2}{4}\int d\mathbf{r}_{23}\delta(r_{23}-1)\left[\frac{\Sigma(r_{23})}{S}\right], \tag{31}$$

where $\Sigma(r)$ is the area of the intersection between the exclusion disks of two particles whose centers are separated by a distance r (see Appendix A). A simple calculation gives that, for $r=1$, $\Sigma(1)=2(\pi/3-\sqrt{3}/4)$, and Eq. (31) is equal to

$$a(1-a)\frac{\pi^2}{16}\rho^2\left[\frac{16}{3}-\frac{4\sqrt{3}}{\pi}\right] . \tag{32}$$

Details of the calculation for the ρ^3 term of Eq. (26) are given in Appendixes B and C. Finally, collecting all terms of the expansion and introducing the coverage $\theta=\rho/\pi/4$ [we redefine accordingly the unit of time by multiplying by $\pi/4$ such that $d\theta/dt=\Phi(a,\theta)$], one obtains

$$\Phi(a,\theta)=1+4(a-1)\theta+\left[\frac{6\sqrt{3}}{\pi}+a\left[\frac{16}{3}-\frac{10\sqrt{3}}{\pi}\right]+a^2\left[-\frac{16}{3}+4\frac{\sqrt{3}}{\pi}\right]\right]\theta^2$$
$$+\left[\left[\frac{40\sqrt{3}}{3\pi}-\frac{176}{3\pi^2}\right]+a\left[\frac{376}{27}-\frac{488\sqrt{3}}{9\pi}+\frac{1834}{9\pi^2}\right]+a^2\left[-\frac{920}{27}+\frac{532\sqrt{3}}{9\pi}-\frac{228}{\pi^2}\right]\right.$$
$$\left.+a^3\left[\frac{496}{27}-\frac{200\sqrt{3}}{9\pi}+\frac{24}{\pi^2}\right]\right]\theta^3+\cdots . \tag{33}$$

One can easily check that for $a=1$ (simple BD) the first- and second-order terms of the expansion vanish, expressing the impossibility of rejecting a particle when a particle touches only two particles before reaching the surface. The θ^3 term for $a=1$ is slightly different from that given by Thompson and Glandt [16]: the numerical value is $-9.949\,78$—instead of $-9.612\,05$. This discrepancy results from a mistake made by Thompson and Glandt in handling the triplet-distribution function. A comparison between the low-coverage expansion and computer simulation is presented in Sec. IV.

III. ASYMPTOTIC KINETICS

An examination of the configurations of adsorbed spheres near the saturation coverage shows that the surface available for adding new particles is made of small isolated targets, in which only a particle can be placed. In RSA ($a=0$), each target can be characterized by one single-length scale parameter h [23,24]; this assumption, which leads to a power-law asymptotic behavior that is well supported by the simulations results [25–27], is closely related to the fact that the minimum area of a target (which is zero in continuum RSA) is reached when h goes to zero, whatever the detailed configuration of the surrounding spheres.

For the ballistic deposition model, an adsorption event can occur either by direct deposition or by rolling motion on the preadsorbed particles. Because of the latter possibility, the smallest target areas are never equal to zero (when $a>0$), which leads, as shown below, to an exponential asymptotic behavior. For times long enough, the direct deposition becomes marginal (the case $a=0$ is not considered in the following) and the relevant target area is that of the surface determined by the centers of the preadsorbed spheres over which the trial sphere may roll to reach the adsorbing surface. Targets can be classified according to the number of such preadsorbed spheres. But contrary to a RSA process, next-neighboring spheres can be involved in an adsorption event. Figure 2 displays some typical targets. Indeed, a target defined by n preadsorbed spheres must be surrounded by "stable" positions corresponding to (potential) second-layer formation; otherwise, more preadsorbed spheres would be involved in the definition of the target: the surface is a convex polygon in which any landing trial particle will eventually be adsorbed.

It is important to note that there is a finite difference between the smallest area of a target defined by three spheres and that of a target defined by four spheres; this is of course also true for targets defined by even more preadsorbed spheres. The smallest target defined by three spheres is equal to $S_{3m}=\sqrt{3}/2$ whereas the smallest target defined by four spheres is equal to $S_{4m}=3\sqrt{3}/4$. As a result, the asymptotic behavior is only determined, as far the leading term is concerned, by the filling of the triangular targets. Characterizing the targets by the area relative to the minimum value $s=S-S_{3m}$, the density $n(s,t)$ of such targets evolves in the asymptotic regime $t\geq t_c$, according to

$$\frac{d}{dt}n(s,t)=-a\frac{4}{\pi}(S_{3m}+s)n(s,t) , \tag{34}$$

where one neglects the filling by direct deposition. The factor $4/\pi$ comes from the new definition of the unit of time introduced in the preceding section. Integrating Eq. (34) gives

$$n(s,t)=n(s,t_c)e^{-a4/\pi(S_{3m}+s)(t-t_c)} . \tag{35}$$

The asymptotic behavior of the coverage is obtained by considering all targets and this yields

$$\theta(a,\infty)-\theta(a,t)\simeq\frac{\pi}{4}\int_0^{s_c}ds\, n(s,t_c)e^{-a4/\pi(S_{3m}+s)t}$$
$$t\rightarrow+\infty , \tag{36}$$

where s_c is an irrelevant upper cutoff.

When $s \to 0$, we assume an analytical expansion of the density of targets,

$$n(s,t_c)=n(0,t_c)+\left[\frac{dn}{ds}\right]_{s=0} s+\cdots . \tag{37}$$

When $s=0$, it is impossible to find a stable position on the other side of the longest segment of the triangle, and the target is no longer defined by only three adsorbed spheres, but at least four [17]. As a consequence, the density of targets vanishes when s goes to zero: $n(0,t_c)=0$. As s and $n(s,t_c)$ are positive numbers, $(dn/ds)_{s=0}$ is also positive; assuming in addition that the derivative is different from zero, the asymptotic behavior is given by

$$\theta(a,\infty)-\theta(a,t)\sim\int_0^{s_c} ds\, s e^{-a4/\pi(S_{3m}+s)t} . \tag{38}$$

Taking the limit of large upper cutoff, we integrate the above equation, which leads to

$$\theta(a,\infty)-\theta(a,t)\sim\frac{e^{-a4/\pi S_{3m}t}}{a^2t^2}\sim\frac{e^{-a2\sqrt{3}/\pi t}}{a^2t^2} . \tag{39}$$

As previously mentioned, the fact that the minimum target area is nonzero leads indeed to an exponential approach towards the jamming limit for $a>0$, whereas in RSA ($a=0$) the approach is algebraic. By refining previous arguments, we now show that the discontinuity when

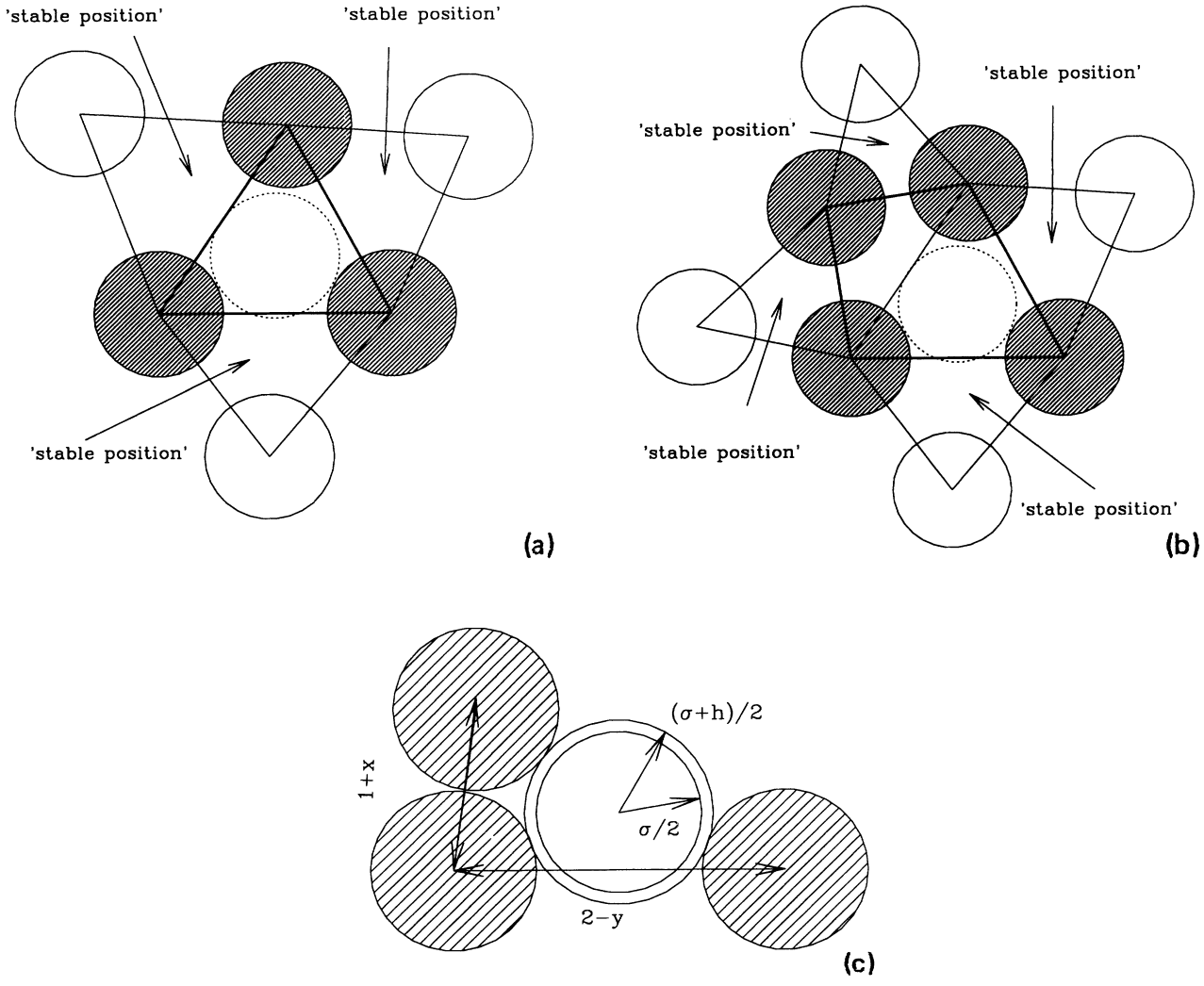

FIG. 2. Available surface area in the asymptotic regime: representative targets defined by (a) three preadsorbed spheres (hatched disks) and (b) four preadsorbed spheres (hatched disks). The target area is delimited by the thick lines and the dashed circles indicate the incoming sphere. (c) Geometry of the smallest targets. The minimum area is obtained for $h=x=y=0$. The dashed circle corresponds to the largest disk that could be inserted. For small values of the parameters, the available area is $S_3=(\sqrt{3}/2)+1/2\sqrt{h+y}+(\sqrt{3}/12)x+\cdots$.

$a \to 0$ is only apparent, and that successive asymptotic regimes appear in this limit.

In the remainder of the section, we consider the case when a becomes very small. In this situation, the targets that remain at long times need to be characterized by more than the surface area available for insertion of a new sphere by rolling. One must also consider the length scale h that can be defined as the difference between the diameter of the largest disk that could be inserted in the target and the diameter of the actual spheres: h is the relevant parameter for describing insertion of a new sphere by direct deposition.

The rate at which a target characterized by h and a set of (unspecified) parameters $\{x\}$ (including, e.g., the numbers of preadsorbed spheres required to define the polygon available for deposition by rolling mechanism) vanishes is then equal to $4/\pi(aS(\{x\},h)+(1-a)C(\{x\})h^2 + O(h^3))$, where S is the area of the polygon available for deposition by rolling and $C(\{x\})h^2$ is the area of the small surface available for direct deposition. Then, the approach to saturation is described by a generalization of Eq. (36) for $a \ll 1$:

$$\theta(a,\infty)-\theta(a,t) \simeq \frac{\pi}{4}\int_0^{h_c} dh \int_0^{\{x\}_c} d\{x\} n(\{x\},h,t_c) e^{-(4/\pi)(aS(\{x\},h)+(1-a)C(\{x\})h^2)t}, \quad t \gg t_c \ . \tag{40}$$

The targets can now be divided into three classes: those that are predominantly destroyed by direct deposition, those that are predominantly destroyed by rolling mechanism, and those for which the two mechanisms have comparable contributions. Since $S(\{x\},h)$ is always larger than $S_{3m}=\sqrt{3}/2$, the first class is characterized by $h \gg \sqrt{a}$. Notice also that the destruction of a target by rolling mechanism becomes effective only for times of the order $1/a$ or larger. For $t_c \ll t \ll 1/a$, the targets with $h < \sqrt{a}$ are almost unaffected, whereas the targets with $h > \sqrt{a}$ vanish because of direct deposition, just like in RSA. As a result,

$$\theta(a,\infty)-\theta(a,t) \sim \frac{K(a)}{\sqrt{t}} + K'(a) \quad \text{if } t_c \ll t \ll 1/a \ , \tag{41}$$

where $K(a)$ goes to a nonzero limit and $K'(a)$ goes to zero when $a \to 0$. For t larger than $1/a$, the rolling mechanism becomes more and more efficient and, again by virtue of the finite, nonvanishing value of S, the kinetics crosses over to an exponential behavior. However, one does not immediately recover the asymptotic behavior given by Eq. (39). The first reason is that it may take some time for the deposition process by rolling to fill the largest targets first so that the remaining targets are predominantly defined by three preadsorbed spheres (this is expected to be true for $t \gg 1/a$); but, in addition, when a becomes very small there may still be a competition between filling by direct deposition and filling by rolling mechanism, even for $h < \sqrt{a}$. Consider for instance targets defined by three preadsorbed spheres. Then the rate of destruction can be written as $a(S_{3m}+s(\{x\},h)) + C(\{x\})h^2$ and it is only for $s(\{x\},h) \gg C(\{x\})h^2$ that one recovers the previously derived behavior, Eq. (39). By considering the geometry of the smallest targets [see Fig. 2(c)] and averaging over nonrelevant parameters, a crude estimate gives $s(\{x\},h) \sim \sqrt{h}$, which implies that the rolling mechanism only dominates when $s \ll a^{1/3}$. The corresponding crossover time is obtained for $ast \sim 1$ when $s \sim a^{1/3}$, i.e., $t \sim a^{-4/3}$, so that one finally has

$$\theta(a,\infty)-\theta(a,t) \sim K'' \frac{e^{-2\sqrt{3}/\pi at}}{(at)^2} \ , \quad t \gg 1/a^{4/3} \ , \tag{42}$$

where K'' is a function of a. The asymptotic kinetics when $a \ll 1$ are thus characterized by three successive regimes and when $a \to 0$ the last two of these shrink and start an infinitely long times so that only the RSA-like behavior survives.

IV. SIMULATION RESULTS AND DISCUSSION

In the simulations, spheres of diameter σ are incident on a square cell of side L. Periodic boundary conditions were employed to eliminate edge effects. The size of the system is specified by the cross-sectional area of one sphere relative to the cell area, $r_a = \pi\sigma^2/4L^2$. The simulations performed to investigate the asymptotic kinetics used a value of 10^{-5} for this parameter and between 200 and 700 independent runs. The short-time behavior was studied with more independent runs, i.e., 50 000 runs. If N denotes the number of adsorbed particles, the coverage is defined as $\theta = N\pi\sigma^2/4L^2$. One simulation consists of a (large) number of attempts to add particles to the surface. At each attempt, the algorithm proceeds as follows. First a trial position within the cell is generated using a uniform random number generator. A check for overlap between the projection of the spheres in the plane, taking proper account of the periodic boundary conditions, is then performed. If no overlap is detected, a uniform random number, ξ, is generated on the interval [0,1]. If $\xi < p$, the trial position is accepted, otherwise it is rejected. This procedure amounts to accepting the directly deposited particle with probability p. If overlap is detected in the initial position, the rolling mechanism is initiated. Physically, this corresponds to following the path of steepest descent of the incoming sphere over those that are already adsorbed. Computationally, this calculation is very time consuming but fortunately it may be replaced by a sequence of restructured positions of the projection of the sphere in the plane. In this way, the three-dimensional process is mapped to a two-dimensional one. Full details are given elsewhere [16,17]. If, after any displacement in the restructuring sequence, no overlap results, the sphere has reached the surface. If overlap is still detected after the fourth displacement, the sphere has failed to reach the surface and is rejected. If the

sphere does reach the surface via the rolling mechanism, it is accepted with probability $p'=1-p$ in the manner described above (without loss of generality, we have chosen p and p' such that $p+p'=1$). In practice, this calculation is performed first; the rolling sequence is computed only if the final position would be accepted. A flow diagram is shown in Fig. 3. If N_a attempts have been made, the elapsed time is defined as $t=pN_a\pi\sigma^2/4L^2$.

In order to verify our result for the coefficient of θ^3 in the case $a=1$, we have plotted the function $Y=4(t-\theta(t))/t^4$, which is related to the number of unsuccessful trials, in Fig. 4. Although large fluctuations are apparent for the shortest times, where almost all of the attempts are successful, a distinct linear region is apparent for larger times. The intercept and slope of this line are equal to the t^3 coefficient and $\frac{5}{4}$ of the t^4 coefficient of $-\Phi(a=1,t)$, respectively. From a least-squares fit of the simulation data, we obtain an intercept of 9.9 ± 0.1 and a slope of -10.5 ± 0.2. The corresponding values of the θ^3 and θ^4 coefficients of $\Phi(a=1,\theta)$ are thus -9.9 ± 0.1 and 13.2 ± 0.2, respectively. The former agrees more closely with our theoretical value of $-9.949\,78$ than with the value quoted by Thompson and Glandt [16], $-9.612\,05\ldots$.

In Fig. 5 we show the simulated rate of deposition $\Phi(a,\theta)$ together with the low-coverage expansion, Eq. (33), to order θ^3. For $a=0$, the low-coverage expansion accounts for most of the behavior of Φ, but the agreement deteriorates with increasing a. For $a\geq1$, it accounts only for the early part of the curve ($\theta<0.15$). Note that for $a\geq1$, Φ is not a monotonically decreasing function of θ, but passes through a maximum that has a larger value than 1. This behavior is due to the choice of time units (in units $kp\tau$, Φ is *not* the probability of adsorption and therefore may be larger than 1), and the maximum is physically related to the increasing efficiency of the rolling mechanism [see Eq. (2)]. The rate of adsorption via rolling initially *increases* with coverage, and when a is larger than 1 this effect dominates the decrease of the available surface for direct deposition due to exclusion effects.

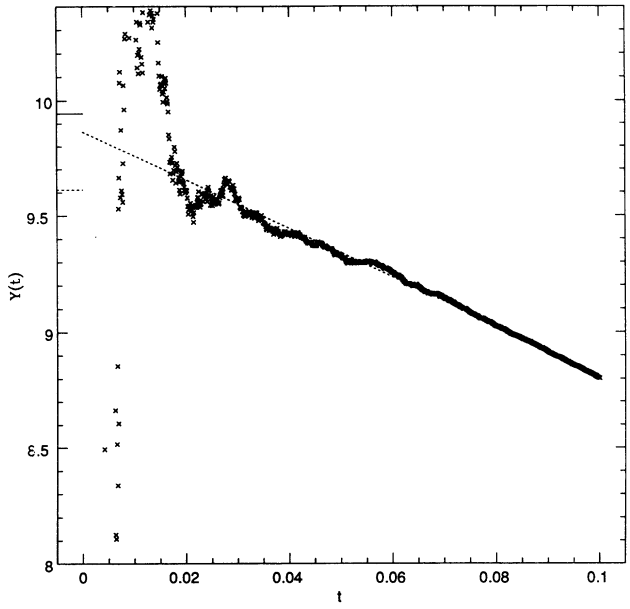

FIG. 4. Plot of $Y(t)=4(t-\theta(t))/t^4$ versus t at short times for $a=1$ (simple BD). The dashed line is a least-squares fit of the simulation data for $t\geq0.03$. The slope and intercept of this line are -10.5 ± 0.2 and 9.9 ± 0.1, respectively. The latter, which is minus the θ^3 coefficient of $\Phi(a=1,\theta)$, agrees more closely with our theoretical estimate (shown as a short, continuous horizontal line) than with that of Thompson and Glandt (short, dashed horizontal line) (see text).

For the simple ballistic deposition model, see Ref. [17], we plotted different functions to check the validity of the predicted asymptotic behavior with exponents $2\sqrt{3}/\pi$ (exponential) and -2 (power law) for $a=1$. In the previous section, we have shown that, for this generalized ballistic deposition model, the final regime of the asymp-

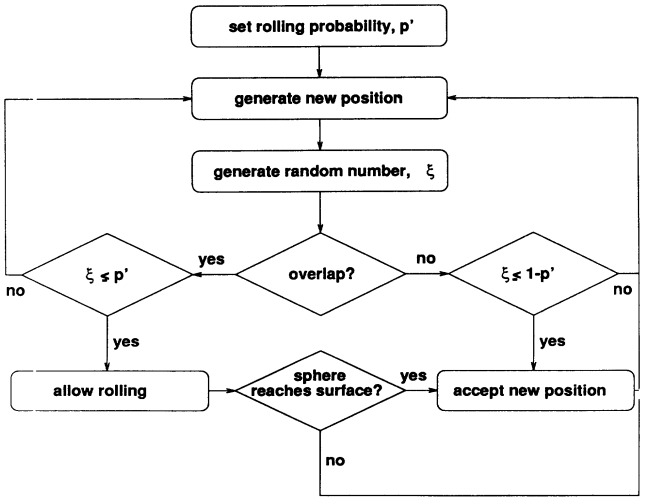

FIG. 3. Flow chart of the simulation algorithm.

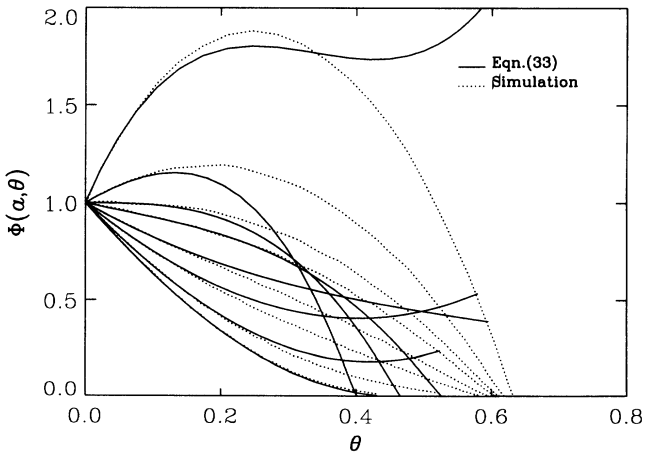

FIG. 5. Rate of deposition $\Phi(a,\theta)$ versus θ for $a=0,0.1,0.3,0.5,0.8,1.0,1.5,3.0$ (from bottom to top on the left-hand side). The continuous lines correspond to the low-coverage expansion [Eq. (33)] and the dashed lines are the computer simulation values.

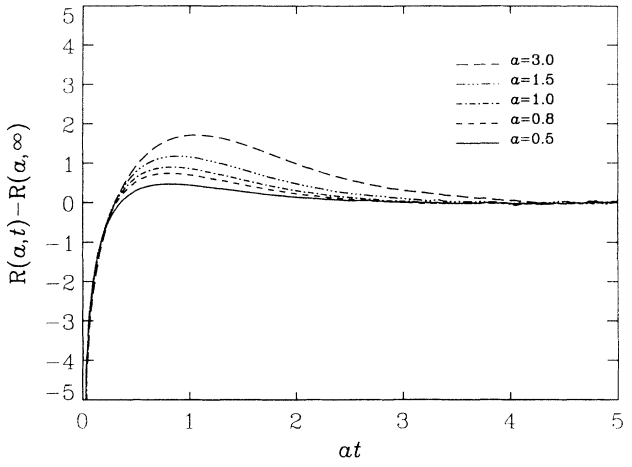

FIG. 6. Asymptotic kinetics: the residual function $R(a,t)=\ln[(\theta(a,\infty)-\theta(a,t))\exp(2\sqrt{3}/\pi at)(at)^2]$ minus its plateau value $R(a,\infty)$ is plotted versus at for $a=0.5,0.8,1.0,1.5,3.0$. The plateau values are given in Table I.

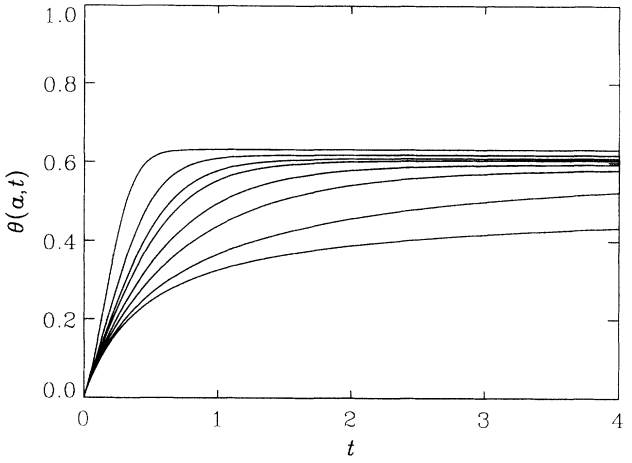

FIG. 7. Coverage $\theta(a,t)$ as a function of time for $a=0,0.1,0.3,0.5,0.8,1.0,1.5,3.0$ (from bottom to top).

totic kinetics is given by a simple scaling form, Eq. (39), with, however, an amplitude that depends on a [see Eq. (42)]. We thus show a master plot of the asymptotic kinetics for various values of a (0.5, 0.8, 1.0, 1.5, 3.0). We introduce the residual function $R(a,t)=\ln[(\theta(a,\infty)-\theta(a,t))\exp(2\sqrt{3}/\pi at)(at)^2]$, and the difference $R(a,t)-R(a,\infty)$ is plotted versus at in Fig. 6. The curves all go to zero for $at>4$, confirming Eq. (39). The plateau values, $R(a,\infty)$, for different a's are presented in Table I. As in the $(1+1)$-dimensional model [18], the plateau value is a function of a, but the dependence cannot be derived by simple analytical arguments. It requires detailed information on the structure of the targets close to the saturation state (compare, e.g., with Eq. (42), $R(a,\infty)=\ln[K''(a)]$). The trend that seems to be satisfied is that the contribution of the last asymptotic regime decreases when a decreases.

In Fig. 7, we display the time dependence of the coverage for several values of a. For increasing a's one observes that the saturation coverage increases (see also Table II) and is reached more rapidly.

With low- and high-coverage regimes in hand, it is useful to combine them to provide an approximate description of the kinetics over the entire range and to predict the saturation coverage. Many authors [27–30] have proposed such treatment for RSA kinetics. The predicted jamming limit for disks, 0.553, compares well with the value from simulation, 0.547 [28]. The corresponding values for the addition of hard spheres to a volume are 0.365 (estimate) and 0.382 (simulation) [27]. Dickman, Wang, and Jensen [30] used the low-coverage series in time in conjunction with the asymptotic power law for disks to construct Padé approximants which yielded an excellent prediction of the jamming limit (0.547 88). Unfortunately, as already shown for the simple ballistic deposition model [17], none of these procedures provides a good estimate for the ballistic deposition saturation coverage. Using the low-coverage expansion up to θ^3 and the asymptotic expression, the method of Dickman, Wang, and Jensen gives a saturation coverage of 0.9 for $a=1$ (instead of 0.61) and similarly poor estimates for other values of a. The reason for this poor performance is likely due to the fact that both the low- and high-coverage expressions have a limited range of validity. To illustrate this point, we have used for $a=1$ the additional θ^4 coefficient of the coverage expansion of Φ estimated from the least-squares fit in Fig. 3. The best results from the interpolants suggested in Ref. 17 and from those of Dickman, Wang, and Jensen are 0.65 and 0.70, respec-

TABLE I. Plateau value, $R(a,\infty)$, of the residual function.

a	$R(a,\infty)$
0.5	−3.43
0.8	−3.25
1.0	−3.18
1.5	−3.02
3.0	−2.75

TABLE II. Saturation coverage $\theta(a,\infty)$ for different values of a. The standard deviation over all runs is equal to 0.006.

a	$\theta(a,\infty)$
0	0.547
0.1	0.5682
0.3	0.5866
0.5	0.5964
0.8	0.6059
1.0	0.6105
1.3	0.6157
1.5	0.6191
2.0	0.6245
2.5	0.6286
3.0	0.6323
4.0	0.6374
5.0	0.6413

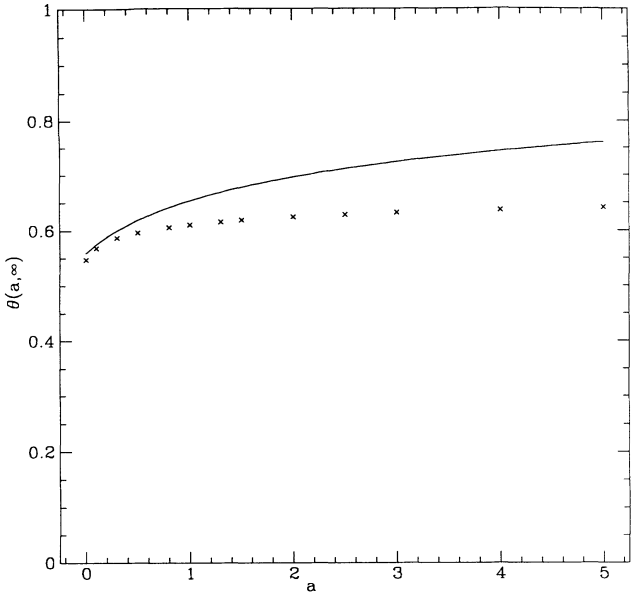

FIG. 8. Saturation coverage as a function of a (crosses). Comparison with a Palásti-like formula (continuous line).

tively, and are indeed closer to the numerical value.

Since we have obtained analytically the exact solution of the generalized ballistic deposition process on a line [18], it is interesting to try a Palásti-like approximation [31–33] in which a simple estimate for the saturation coverage on a plane [(2+1)-dimensional system] is provided by the square of the value on a line [(1+1)-dimensional process]:

$$\theta_{2+1}(a;\infty)\approx(\theta_{1+1}(a;\infty))^2 . \tag{43}$$

The results of this approximation, which we stress have no sound theoretical basis when applied to the present problem, are shown in Fig. 8. The approximation is very good for RSA ($a=0$), 0.558 instead of 0.547, but its quality decreases as a increases. For example, for $a=1$ it gives 107% of the exact result and for $a=3$, 114%. Overall, the Palásti construction predicts the correct trend with increasing a, but, of course, it predicts a maximum value of 1, which is physically unrealistic. The actual value should be less than the coverage at random close packing, 0.82 [34].

V. CONCLUSION

In this paper, we have investigated an irreversible-deposition model that generalizes both random sequential adsorption and ballistic-deposition models by including restructuring effects. Monolayer formation is controlled by one parameter that sets the relative rate of the two mechanisms of deposition, i.e., direct deposition and the rolling mechanism. By means of liquid-state methods, the third-order density expansions for the pair-density function and for the rate of deposition have been obtained, which provides an exact description of the kinetics and the structure at short times. An analytical expression for the asymptotic kinetics has been also derived. The computer simulations show a good agreement with the predicted results. Although the results presented in this paper apply for any value of a, they are most useful for a not much larger than 1. For $a\simeq 3$, a percolating structure is observed. The structural properties are therefore significantly different and the model is best analyzed using other approaches, e.g., percolation theory. A detailed investigation of the nature of the percolation transition is under way.

ACKNOWLEDGMENTS

This work has been supported in part by NATO (Grant No. 890872). The Laboratoire de Physique Théorique des Liquides is Unité de Recherche Associée No. 765 au Centre National de la Recherche Scientifique.

APPENDIX A

We have to calculate integrals like

$$I=\int\int d2\,d3\,f_{12}f_{13}G(2,3) , \tag{A1}$$

where $G(2,3)$ only depends upon the relative distance r_{23}. Using the property of uniformity, the above integral can be rewritten as

$$I=\frac{1}{S}\int\int\int d1\,d2\,d3\,f_{12}f_{13}G(2,3) , \tag{A2}$$

where S is the total area of the system. We now introduce the function $\Sigma(r_{23})$ such that

$$\Sigma(r_{23})=\int d1\,f_{12}f_{13} . \tag{A3}$$

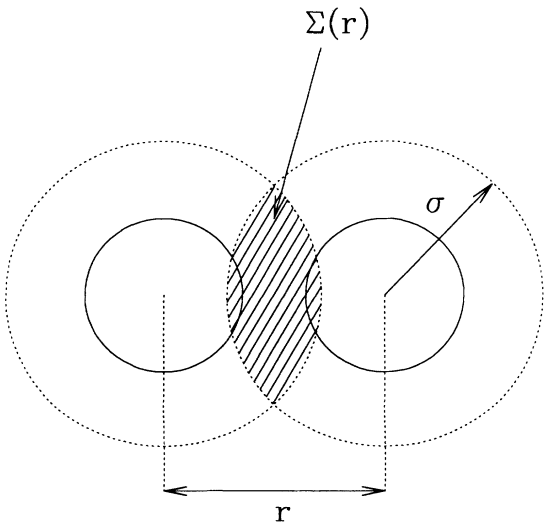

FIG. 9. Intersection of the exclusion disks of two particles whose centers are separated by a distance r.

The function $\Sigma(r)$ has a simple geometrical interpretation: it is the area of intersection between the exclusion disks of two particles whose centers are separated by a distance r (see Fig. 9). An elementary calculation gives

$$\Sigma(r)=2\left[\alpha(r)-\frac{\sin(2\alpha(r))}{2}\right], \tag{A4}$$

where $\alpha(r)$ is the angle between $\mathbf{r}_{12}$ and $\mathbf{r}_{13}$. Changing the variables from $(\mathbf{r}_2,\mathbf{r}_3)$ to $(\mathbf{r}_2,\mathbf{r}=\mathbf{r}_2-\mathbf{r}_3)$, Eq. (A2) becomes

$$I=\frac{1}{S}\int d\mathbf{r}\,\Sigma(r)G(r)$$

$$=\frac{2\pi}{S}\int dr\,r\Sigma(r)G(r)\ . \tag{A5}$$

APPENDIX B: CALCULATION OF THE ρ^3 TERM OF EQ. (26)

The third-order term of the expansion of $\Phi(a,\rho)-(1-a)\Phi(a=0,\rho)$ is the sum of the two following contributions:

$$\mathcal{I}(a,\rho)=(1-a)\frac{\rho^3}{6}\int\int\int d2\,d3\,d4\,f_{12}f_{13}f_{14}(g_3^{(0)}(2,3,4;a)-g_3^{(0)}(2,3,4;0)) \tag{B1}$$

and

$$\mathcal{J}(a,\rho)=-\frac{a}{6}\rho^3\int\int\int d2\,d3\,d4\frac{A(2,3,4)}{S}g_3^{(0)}(2,3,4;a)\ . \tag{B2}$$

We introduce the function $\Sigma(2,3,4)=-\int d1\,f_{12}f_{13}f_{14}$, which represents the area of the intersection between the exclusion disks around particles whose centers are located in $\mathbf{r}_2,\mathbf{r}_3,\mathbf{r}_4$ (see Fig. 10). By using Eq. (28), introducing the coverage $\theta=\pi/4\rho$, and relabeling the integration variables, one then obtains

$$\mathcal{I}(a,\theta)=-(1-a)\frac{32\theta^3}{3\pi^2 S}\int\int\int d1\,d2\,d3[\Phi^{(2)12|3}(1,2,3;a)-\Phi^{(2)12|3}(1,2,3;0)]\Sigma(1,2,3)\ . \tag{B3}$$

Considerations of symmetry lead us to choose $r_{12}=1$ and to use as variables either $(s=r_{13},\ t=r_{23})$ or $(s=r_{13},\alpha)$, α being the angle between $\mathbf{r}_{12}$ and $\mathbf{r}_{13}$. By means of those variables, the function $\Sigma(1,2,3)$ can be expressed as follows [35]: for $1\le s\le\sqrt{2+\sqrt{3}}$ and for $\cos^{-1}(1/(2s))\le\alpha\le\pi/3+\cos^{-1}(s/2)$,

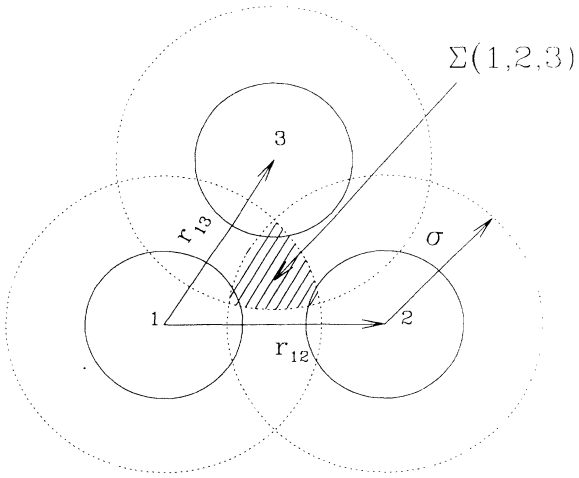

FIG. 10. Intersection of the exclusion disks of three particles centered in 1,2,3.

$$\Sigma(1,s,\alpha)=-\frac{\pi}{6}-\frac{\sqrt{3}}{4}+\cos^{-1}\left[\frac{s}{2}\right]-\frac{s}{2}\left[1-\frac{s^2}{4}\right]^{1/2}$$

$$+\cos^{-1}\left[\frac{t}{2}\right]-\frac{t}{2}\left[1-\frac{t^2}{4}\right]^{1/2}+\frac{s}{2}\sin(\alpha)\ , \tag{B4}$$

t and α being related by $t=\sqrt{1+s^2-2s\cos\alpha}$. For $1\le s\le\sqrt{3}$ and for $[\pi/3+\cos^{-1}(s/2)]\le\alpha\le\cos^{-1}[(s^2-3)/(2s)]$,

$$\Sigma(1,s,\alpha)=2\cos^{-1}\left[\frac{t}{2}\right]-t\left[1-\frac{t^2}{4}\right]^{1/2}\ . \tag{B5}$$

Combining Eqs. (29), (B3), (B4), and (B5), the following expression for $\mathcal{I}(a,\theta)$ is obtained after some algebraic manipulations:

$$\mathcal{I}(a,\theta)=-\theta^3\frac{128}{3\pi^2}(1-a)\{I_+ +I'_{++}+I''_{++}+I_{+++}\}\ , \tag{B6}$$

where

$$I_+=3a\left\{\int_1^{\sqrt{2+\sqrt{3}}}ds\,s\int_{\cos^{-1}[1/(2s)]}^{\pi/3+\cos^{-1}(2s)}d\alpha\frac{\Sigma(1,s,\alpha)}{S}\right.$$

$$\left.+\int_1^{\sqrt{3}}ds\,s\int_{\pi/3+\cos^{-1}(2s)}^{\cos^{-1}[(s^2-3)/(2s)]}\frac{\Sigma(1,s,\alpha)}{S}\right\}, \tag{B7}$$

$$I'_{++}=\frac{a^2}{2}\int_1^2 dt\frac{t}{\sin\alpha(1,s,t)}\frac{\Sigma(1,s,t)}{S}\ , \tag{B8}$$

$$I''_{++}=\frac{a}{2}\int_1^2 dt\ t\sin\alpha(1,s,t)\frac{\Sigma(1,s,t)}{S}\ , \tag{B9}$$

$$I_{+++}=\frac{3a^2}{8\sqrt{3}}\frac{\Sigma(1,1,1)}{S}\ . \tag{B10}$$

Performing all integrations leads to

$$I_{+}=a\left[-\frac{\pi^2}{12}-\frac{\sqrt{3}\pi}{16}+\tfrac{51}{32}\right]\ , \tag{B11}$$

$$I'_{++}=a^2\left[\frac{7\pi^2}{72}-\frac{\sqrt{3}\pi}{12}+\tfrac{1}{4}\right]\ , \tag{B12}$$

$$I''_{++}=a\left[\frac{7\pi^2}{144}-\frac{\sqrt{3}\pi}{96}-\tfrac{19}{96}\right]\ , \tag{B13}$$

$$I_{+++}=\frac{a^2}{16}(\pi\sqrt{3}-3)\ . \tag{B14}$$

We now proceed to a similar treatment for $\mathcal{I}(a,\theta)$:

$$\mathcal{I}(a,\theta)=-a\frac{32\theta^3}{3\pi^2}\times\int\int\int d1\,d2\,d3\,\Phi^{(2)12|3}(1,2,3;a)\frac{A(1,2,3)}{S}\ . \tag{B15}$$

$A(1,2,3)$ is the area of the triangle formed by the centers of particles 1, 2, and 3 such that every particle center landing above this triangle reaches a stable elevated position (corresponding to a second layer); consequently, this triangle is not obtuse and its circumradius r_c is less than the diameter of a sphere. Then, $A(1,2,3)$ is equal to zero, except for $\alpha\le\pi/2$ and $r_c=r_{23}/\sin\alpha\le 1$ where one has

$$A(1,2,3)=\tfrac{1}{2}r_{12}r_{13}\ . \tag{B16}$$

Using Eqs. (29) and (B4), $\mathcal{I}(a,\theta)$ can be rewritten as

$$\mathcal{I}(a,\theta)=-a\theta^3\frac{128}{3\pi^2}\{J+J_{+}+J'_{++}+J''_{++}+J_{+++}\}\ , \tag{B17}$$

where

$$J=3\left\{\int_1^{\sqrt{2}}dr\,r^2\int_r^{\sqrt{4-r^2}}ds\,s^2\int_{\cos^{-1}[r/(2s)]}^{\pi/2}d\alpha\sin(\alpha)+\int_1^{\sqrt{2}}dr\,r^2\int_r^{\sqrt{2+\sqrt{4-r^2}}}ds\,s^2\int_{\cos^{-1}(r/(2s))}^{\cos^{-1}\{[sr-\sqrt{(4-r^2)(4-s^2)}]/4\}}d\alpha\sin(\alpha)+\int_{\sqrt{2}}^{\sqrt{3}}dr\,r^2\int_r^{\sqrt{2+\sqrt{4-r^2}}}ds\,s^2\int_{\cos^{-1}[r/(2s)]}^{\cos^{-1}\{[sr-\sqrt{(4-r^2)(4-s^2)}]/4\}}d\alpha\sin(\alpha)\right\}\ ,$$

$$=\frac{31}{64}+\frac{\sqrt{3}\pi}{32}+\frac{\pi^2}{24}\ , \tag{B18}$$

$$J_{+}=\frac{3}{2}a\left\{\int_1^{\sqrt{3}}ds\,s^2\int_{\cos^{-1}[1/(2s)]}^{\pi/2}d\alpha\sin\alpha+\int_{\sqrt{3}}^{\sqrt{2+\sqrt{3}}}ds\,s^2\int_{\cos^{-1}(1/(2s))}^{\cos^{-1}(s/4-\sqrt{3(4-s^2)}/4)}d\alpha\sin\alpha\right\}\ ,$$

$$=a\left[\frac{9}{16}+\frac{\sqrt{3}\pi}{16}\right]\ , \tag{B19}$$

$$J'_{++}=\frac{a^2}{4}\int_{\pi/3}^{\pi/2}d\alpha\sin\alpha\ ,$$

$$=\frac{a^2}{8}\ , \tag{B20}$$

$$J''_{++}=\frac{a}{4}\int_{\pi/3}^{\pi/2}d\alpha\sin^3\alpha\ ,$$

$$=\frac{11a}{96}\ , \tag{B21}$$

$$J_{+++}=\frac{3a^2}{16}\int_1^2 dt\ t\frac{\delta(t-1)}{2}\ ,$$

$$=\frac{3a^2}{32}a\ . \tag{B22}$$

Combining Eqs. (B6), (B11)–(B14), (B17)–(B22), and previously obtained results for RSA [21] leads to the θ^3 term of Eq. (33).

[1] J. Feder, J. Theor. Biol. **87**, 237 (1980).
[2] J. Feder and I. Giaever, J. Colloid Interface Sci. **78**, 144 (1980).
[3] A. Schmitt, R. Varoqui, S. Uniyal, J. L. Brash, and C. Pusiner, J. Colloid Interface Sci. **92**, 25 (1983).
[4] G. Y. Onoda and E. G. Liniger, Phys. Rev. A **33**, 715 (1986).
[5] Z. Adamczyk, M. Zembala, B. Siwek, and P. Warszýnski, J. Colloid Interface Sci. **140**, 123 (1990).
[6] J. Ramsden, Phys. Rev. Lett. **71**, 295 (1993).
[7] For a comprehensive review, see J. W. Evans, Rev. Mod. Phys. **65**, 1281 (1993).
[8] P. Schaaf, A. Johner, and J. Talbot, Phys. Rev. Lett. **66**, 1603 (1991).
[9] B. Senger, J.-C. Voegel, P. Schaaf, A. Johner, A. Schmitt, and J. Talbot, Phys. Rev. A **44**, 6926 (1991).
[10] B. Senger, P. Schaaf, J.-C Voegel, A. Johner, A. Schmitt, and J. Talbot, J. Chem. Phys. **97**, 3813 (1992).
[11] B. Senger, F. J. Bafaluy, P. Schaaf, A. Schmitt, and J.-C. Voegel, Proc. Natl. Acad. Sci. U.S.A. **89**, 9449 (1992).
[12] G. Tarjus and P. Viot, Phys. Rev. Lett. **68**, 2354 (1992).
[13] P. Wojtaszczyk, P. Schaaf, and B. Senger (unpublished).
[14] J. Talbot and S. Ricci, Phys. Rev. Lett. **68**, 958 (1992).
[15] R. Jullien and P. Meakin, J. Phys. A **25**, L189 (1992).
[16] A. P. Thompson and E. D. Glandt, Phys. Rev. A **46**, 4639 (1992).
[17] H. S. Choi, J. Talbot, G. Tarjus, and P. Viot, J. Chem. Phys. **97**, 4256 (1993).
[18] P. Viot, G. Tarjus, and J. Talbot, Phys. Rev. E **48**, 480 (1993).
[19] G. Tarjus, P. Schaaf, and J. Talbot, J. Stat. Phys. **63**, 167 (1991).
[20] J. A. Given and G. R. Stell, in *Proceedings of the XVIth International Workshop on Condensed-Matter Theories, June 1992* (Plenum, New York, 1993).
[21] P. Schaaf and J. Talbot, Phys. Rev. Lett. **62**, 175 (1989).
[22] J. A. Given, Phys. Rev. A **45**, 816 (1992).
[23] Y. Pomeau, J. Phys. A **13**, L193 (1980).
[24] R. H. Swendsen, Phys. Rev. A **24**, 504 (1981).
[25] E. L. Hinrichsen, J. Feder, and T. Jøssang, J. Stat. Phys. **44**, 793 (1986).
[26] D. W. Cooper, Phys. Rev. A **38**, 522 (1988).
[27] J. Talbot, P. Schaaf, and G. Tarjus, Mol. Phys. **72**, 1397 (1991).
[28] J. W. Evans, Phys. Rev. Lett. **62**, 2642 (1989).
[29] S. Ricci, J. Talbot, G. Tarjus, and P. Viot, J. Chem. Phys. **97**, 5217 (1992).
[30] R. Dickman, J. Wang, and I. Jensen, J. Chem. Phys. **94**, 8252 (1991).
[31] I. Palásti, Publ. Math. Hung. Acad. Sci. **5**, 353 (1960).
[32] B. J. Brosilow, R. M. Ziff, and R. D. Vigil, Phys. Rev. A **43**, 631 (1991).
[33] B. Bonnier, M. Hontebeyrie, and C. Meyers, Physica A **198**, 7 (1993).
[34] D. Bideau, A. Gervois, L. Oger, and J. P. Troadec, J. Phys. (Paris) **47**, 1697 (1986).
[35] P. C. Hemmer, J. Chem. Phys. **42**, 1116 (1963).